ARCHIVES OF ACOUSTICS
14, 3–4, 261–281 (1989)

ACOUSTIC ACTIVITY OF SOME METALS DETERMINED BY THE ACOUSTIC EMISSION METHOD

S. PILECKI* and J. SIEDLACZEK**

*Institute of Fundamental Technological Research, Polish Academy of Sciences, 00-049 Warsaw, Świętokrzyska 21 (Poland)

**High Pressure Research Center, Polish Academy of Sciences, 01-142 Warsaw, Sokołowska 29 (Poland)

Measurements of the acoustic emission (*AE*) count rate or count sum as well as the *RMS* value have been carried out by the use of the different *AE* analysers and the testing machines. Specimens of the Armco iron, 45 steel, 45 HNMFA steel, bearing steel ŁH15, beryllium bronze BB2 and the alloy of the maraging type N18K9M5T and PA2N alloy have been tested. Two kinds of specimens of St90PA carbon-manganese steel have been tested, too: from new railway rails and from the 10-th year long exploited rails. *AE* characteristics and the results of the Kaiser and Bauschinger effect measurements have been presented.

Pomiary gęstości lub sumy zliczeń emisji akustycznej (*EA*) oraz wartości skutecznej *RMS* zostały wykonane za pomocą różnych analizatorów *EA* i maszyn wytrzymałościowych. Zbadane zostały próbki z żelaza Armco, stali węglowej 45, stali 45HNMFA, stali łożyskowej ŁH15, brązu berylowego BB2, stopu typu maraging N18K9M5T, stopu aluminium PA2N oraz stali węglowo-manganowej St90PA w dwóch odmianach: wykonanych z szyn kolejowych nowych i z szyn wyjętych z toru po 10 latach eksploatacji. Przedstawionio charakterystyki *EA* wszystkich tych materiałów oraz wyniki pomiarów efektu Kaisera i efektu Bauschingera stali St90Pa.

1. Introduction

Acoustic emission (*AE*) results in the propagation of the elastic waves in deformed material due to the release of its locally accumulated elastic energy [1]. *AE* sources can be concerned in three scales, that is: macro, micro and submicro scale. Bibliography of the problem distinguishes several sources of the *AE*, such as: motion of dislocations [1, 2], internal friction, initiation and propagation of crack [3–9], stress corrosion [1] or phase transitions [10]. Motion of dislocations seems to be the most important source of *AE*. It happens because the rest of the above mentioned sources are triggered, in direct as well as in indirect sense, by dislocations. Particularly, the unsteady motion of dislocations is accompanied by acoustic effects. Acoustic activity of the specimen significantly grows with decreasing velocity of dislocations due to the presence of obstacles on their way [1].

Quantitative results of *AE* measurement depend on the kind of tested material, its internal structure, kind and intensity of loading, value of self stresses, state of the interface and on many external factors. Variety of the mechanisms generating the acoustic signal and the influence of many factors causes that every kind of the material as well as the materials of the same chemical composition but of the different grain size or different internal structure, have their individual acoustic characteristics. These characteristics must be recognized before the investigations leading to the formulation of the opinion on the structure and to the estimation ot the structure deformations due to the crack growth, are initiated. In this way before the beginning of the investigations of applicable value concerning structures and machines, *AE* characteristics of their material should be obtained first. These characteristics are next used as the reference base in further tests.

The present paper is the continuation of previous work [1]. Possible differences in *AE* characteristics obtained for different materials are discussed. Possible applications of the *AE* method in determining some properties of the normalized carbon-manganese St90PA steel are also discussed. *AE* measurements for the materials in different state have been conducted during static strength tests. In this number exploited materials of the different age have been tested. In the St90PA steel tests the influence of the experiment conditions on the *AE* results have been verified. Three different test stands existing in two different laboratories have been applied in these works. The significant influence of disturbances both on the experimental results and on the necessity of verification of test apparatuses and conditions is connected with this fact.

2. Test apparatuses

Tests of the *AE* of all investigated materials except of the St90PA steel and the PA2N alloy have been done at the Zentralinstitut fuer Festkoerperphysik und Werkstofforschung of the German Democratic Republic Academy of Sciences in Dresden. Tests have been carried out for the test apparatus composed of the Trodyne *AE* analyser and the Zwick 10T testing machine of the strength power of 100 kN. The *SIMS* (Structural Integrity Monitoring System) module has been the basic element of the apparatus for *AE* measurements. This module contains systems for analog and digital processing of the acoustic signal (Fig. 1). Polish and German piezoelectric resonance transducers, *PP*, have been used in the measurements. Their resonance frequency has been equal to 200 kHz. The *EA* head has been connected with the first preamplifier *PA*1, by a doubly shielded cable of the length of 20 cm. Preamplifier has amplified the input electric signal by 40 dB. The low frequencies of the signal have been eliminated by virtue of the high-pass filter *HPF*. Frequencies lower than 100 kHz have been eliminated. Two independent cables leaded out the signal from the *HPF* filter. Two additional preamplifiers *PA*2 and *PA*3 have been used in secondary amplification of the signal. The *SIMS* system has contained, among the others, the

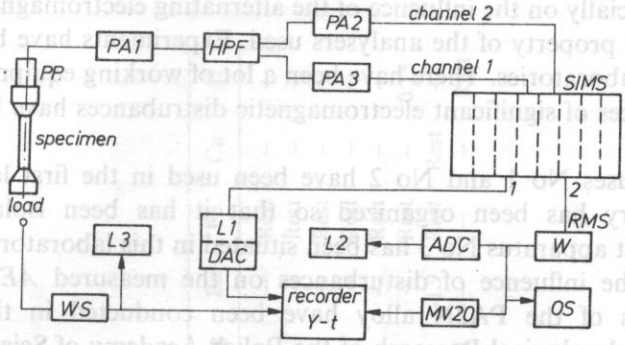

Fig. 1. Block diagram of the *AE* analyser

following equipment: high-pass filters, discriminators and system of the signal processing. These systems have produced classical parameters measured by the *AE* method, such as count rate and count sum, event rate and event sum and the *RMS*, that is root mean square of the acoustic signal. The output No 1 of the *SIMS* system has been giving the signal of the count rate in the digital form. Its value have been visible by use of the *L*1 counter. Next the signal has been passing through the digital-analog converter *DAC*. The converter has been integrated with the *L*1 counter. Then the signal has been registered by a multimanual *y–t* recorder. The averaged acoustic signal has been obtained from the second output channel of the *SIMS* system. This signal has been next amplified by the amplifier *W* and directed to the oscilloscope *OS*, digital-analog converter *DAC*, counter *L*2 and the milivoltmeter MV20 and *y–t* recorder.

Tests of the St90PA carbon-manganese steel have been carried out in Warsaw. The following three test apparatus have been used:

1. Set for *AE* measurements (*AE* analyser) type *E*1 manufactured by Institute of Nuclear Research, Poland, together with the DZM 180 printer and the Instron 1251 testing machine of a hydro drive.

2. Set for *AE* measurements the same as for set-up 1, the mechanical drive testing machine manufactured by Schoper company, German Democratic Republic. Tensile force of this machine has been equal to 100 kN.

3. Set for *AE* measurements type *DEMA*-10 manufactured by ZD Techpan, PAS, Poland, and the hydraulic press of the load 1500 kN colaborating with the reverser manufactured by the High Pressure Center, Unipress, Warsaw.

Acoustic investigations of the St90PA steel have been carried out by using these three test stands. Analogous experimental program has been used every time. Basic *AE* parameters such as count rate, and sum and event rate and events sum (excluding *RMS*) have been determined by employing of the four-channel *AE* analyser type *E*1 and one-channel analyser *DEMA*-10. High sensitivity and the low level of the self-noices are the characteristic properties of these analysers. Their sensitivity is comparable with the sensitivity of the *SIMS* set. Low resistance on the external

disturbances, specially on the influence of the alternating electromagnetic field is also the characteristic property of the analysers used. Experiments have been conducted in two different laboratories. There have been a lot of working equipment in the first laboratory. Sources of significant electromagnetic distrubances have been present in this laboratory.

Test apparatuses No· 1 and No 2 have been used in the first laboratory. The second laboratory has been organized so that it has been isolated from any disturbances. Test apparatus No 3 has been situated in this laboratory what allowed us to estimate the influence of disturbances on the measured *AE* parameters.

Investigations of the PA2N alloy have been conducted in the Institute of Fundamental Technological Research of the Polish Academy of Sciences by the use of the testing machine Instron 1251 and the *AE* analyser manufactured by the French company Audimat P. Because of the worse quality of the Audimat P analyser, manifested mainly in the high level of its self-noices, results obtained by the use of such an analyser cannot be quantitatively compared with other results.

3. Material and testing technique

The following materials have been used in experiments: Armco iron, carbon steel 45, 45HNMFA structural steel, ŁH15 bearing steel, BB2 beryllium bronze, type N18K9M5T maraging dispersion hardening alloy, PA2N aluminium alloy and St90PA carbon-manganese steel of two varieties: new and exploited within 10 years railway rails. Table 1 shows the chemical composition of these materials and Table 2 shows some of their mechanical properties.

Ten or five-times cylindrical specimens as well as flat specimens have been used for tests. The main dimensions of the specimens and way of their attachment in testing machine are shown in Fig. 2a. St90PA steel has been tested for the 10-times specimens on three test stands (see Chapter 2) and the PA2N alloy for flat specimens (Fig. 2b) on the Instron 1251 testing machine. Five-times specimens of the 45HNMFA, ŁH15, BB2 bronze and N18K9M5T alloy have been tensed by the use of Zwick mechanical testing machine. Value of the tensile load has been registered by the pen of the testing machine and together with the *AE* results on the *y–t* plotter. The force signal has been intensified by the *WS* amplifier, Fig. 1, and registered by *y–t* plotter and *L*3 counter. Use of the *L*3 counter allowed the on-line control of tensile force value. *L*3 counter has been used mainly in establishing the initial tension of the specimen after it has been attached to the handles of testing machine. It has been also used to reduce the axial clearance in handles.

Specimens have been stretched in testing machine by the use of the special handles, Fig. 2a, endowed with washers damping mechanical disturbances from mechanical and hydraulic elements of the drive. Stretching rate of the 5-times specimens has been equal 0.5 mm/min and the approximate rate for 10-times specimens was 1 mm/min what corresponds to $2.78 \cdot 10^{-4}\ s^{-1}$ in the relative measure when the active length of the specimen is taken into account.

Table 1. Chemical composition of tested materials

Material	C	Mn	Si	Cr	Ni	Mo	V	S	P	Co	Ti	Mg	Be	Fe	Cu	Al
Armco	0.02	–	–	–	–	–	–	–	–	–	–	–	–	Rest	–	–
45	0.45	0.50	0.30	–	–	–	–	–	–	–	–	–	–	Rest	–	–
St90PA	0.68	1.11	0.24	0.01	0.01	0.10	0.02	0.027	0.026	–	–	–	–	Rest	–	–
45HNMFA	0.45	0.50	0.30	1.00	1.70	0.25	0.15	0.025	0.025	–	–	–	–	Rest	–	–
ŁH15	1.10	0.40	0.30	1.50	0.30	–	–	0.020	0.027	–	–	–	–	Rest	–	–
N18K9M5T	0.012	–	–	–	18.20	4.87	–	–	–	9.0	0.72	–	–	Rest	–	0.13
BB2	–	–	–	–	–	–	–	–	–	0.25	–	–	1.9	Rest	Rest	–
PA2N	–	–	–	–	–	–	–	–	–	–	–	2.8	–	–	–	Rest

Table 2. Mechanical properties of tested materials

Material	σ_{ys} MPa	σ_u MPa	A_5 %	Necking %	Hardness HRC
Armco	155	230	26	65	–
45	327	500	24	60	–
St90PA new	600	1010	10	19	30
St90PA expl.	525	985	10	19	30
45HNMFA	1530	2040	10	32	52
	1375	1500	12	34	42
ŁH15	1780	2470	0.5	–	60
N18K9M5T	1730	1910	10	36	50
BB2	890	1160	2	–	36
PA2N	180	270	–	–	

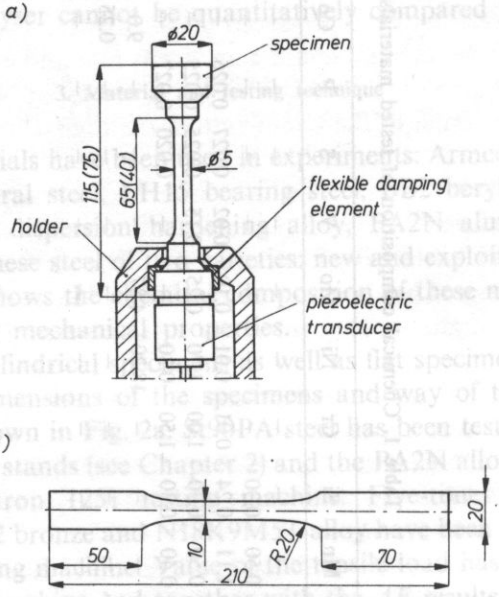

Fig. 2. Specimens for tensile testing: a) Cylindrical specimen in special holder; b) Flat specimen from PA2N alloy

Beam specimens have been used for establishing the characteristics of the St90PA steel in bending. The same specimens have been used in Bauschinger effect investigations. Their dimensions were $20 \times 30 \times 240$ mm^3. Bended specimens have been strained with the velocity of the testing machine traverse shifting equal to 2 mm/min.

In the *AE* analysers type *E*1 and *DEMA*-10, transducers type 0.5LR17B manufactured by Unipan have been used. The amplification of the preamplifier was 40 dB and the transmitted frequency band was 60...250 kHz. Discrimination

level and amplification of the main amplifier were different for each set. Their values are shown in the diagrams presenting the results of the measurements. These parameters have been related to the conditions of external disturbances and to the possibilities of the adaptation to the parameters of the cooperation with another equipment. The *AE* converter and transmitted frequency band have been calibrated experimentally by use of the equipment for *AE* simulation.

4. Acoustic emission characteristics of tested materials

The *AE* characteristics have been obtained for 8 different materials. Taking into account tests of two materials (45 HNMFA and St90PA) with two variations and remembering that one of them has been tested on three apparatus, the total amount of 14 different characteristics has been obtained. At least 5 specimens have been tested for each testing group. Good repeatability of the results obtained for each group has been found. Representative characteristics of all the tested material are presented below.

For most materials the following characteristics have been obtained: tension curve, count rate and *RMS*. In many cases the nature of changes of all the *AE* parameters obtained for the given material is similar. These parameters are count rate and count sum, event rate and event sum and *RMS*. Usually, the parameters like count rate and event rate can be used interchangeably and we can notice that when one of them is known, then the information about the acoustic features of the material is sufficient. On the other hand, there are materials for which differences between characteristics presented in the form of the count rate and *RMS* are appreciable. Results of the *AE* measurements are presented together with loading curves. Both curves have been registered simultaneously and should be interpreted as the inseparable pair when the *AE* characteristics of the materials as well as the Kaiser effect are considered. Certain differences between the obtained loading curves and the ideal curves must be noticed. Ideal curves are obtained when the tensile force and the specimens elongation are registered simultaneous by the tensometer attached to the specimen. These differences can be observed in spite of the fact that in both cases the specimen's loading takes place with the constant velocity of the testing machine traverse shifting. In acoustic tests, specimens are wrestled in the testing machine handles by means of the flexible elements damping external interferences (Fig. 2). It results from this fact that the stiffness of the loading system in tension test is changed and differences in the rate of specimen straining occurs. In the beginning of the loading process mainly more flexible washers are subjected to strain. It reflects at the initial point of the graph as the progressively growing curve. Further, flexibility of the washers decreases and the increase of their strain is transient. Corresponding point of the tension curve is imperceptibly deformed but its accuracy is good enough when the conducted experiments are of the comparative nature. All described process can be pointed out as the source of the differences mentioned above.

Deformation of the flexible washers is sometimes accompanied by a inconspicuous acoustic effect. The *AE* image of the tested materials is not deformed by this effect because it appears only initially for low level of the load, when the proper *AE* phenomenon does not appear. Only part of the stretched specimens has been loaded to the final break oft. It happened because the specimen's break oft is accompanied by a strong shock which, in turn, can lead to destruction of the piezoelectric transducer.

1. Armco iron. *AE* characteristic of the annealed Armco iron consists of two parts differing from each other (Fig. 3). The first part corresponds to the Lüders platform, whereas the second one – to the hardening range. According to the *RMS* curve, very intensive acoustic activity together with the characteristic minima and maxima is observed in the range of the plastic flow. In all the range of the Lüders platform usually 4 maxima and 4 minima can be observed. Beginning of the acoustic activity appears in the range of the elastic deformation and the last minimum always corresponds to the end of the Lüders platform. This end is marked on the tension curve also as the characteristic minimum. The mean increment of the specimen

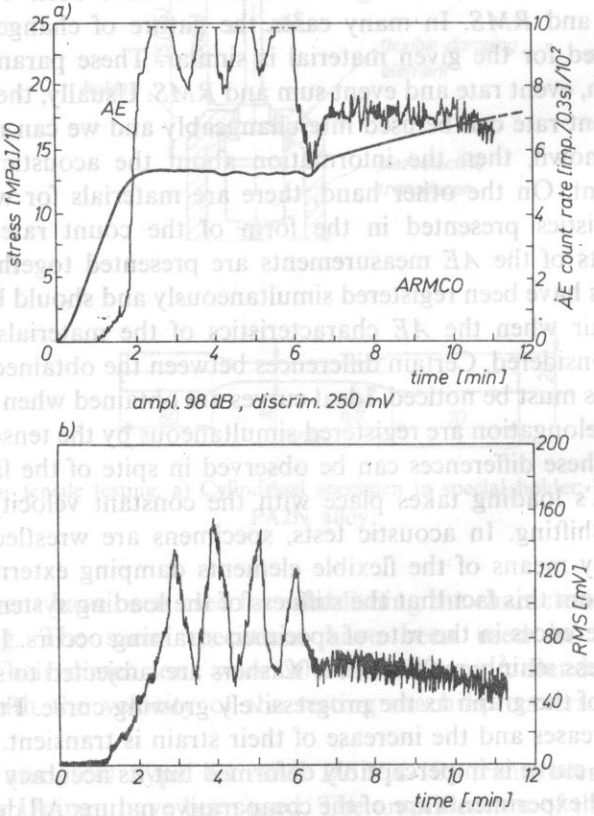

Fig. 3. *AE* characteristic of ARMCO iron: a) loading curve and *AE* count rate; b) *RMS*

elongation measured within the range of the plastic flow of the material has been equal to 3%.

Within the hardening range of the material, acoustic activity initially slightly grows, next monotonically decreases and disappears in the vicinity of the beginning of the specimen necking. The nature of the *AE* count rate curve is similar within the tension range. The average total elongation of the Armco iron specimens measured to their final rupture has been 26% whereas the average reduction of the area of the specimen measured in the fracture mane has been 65%.

2. 45 carbon steel. General character of the results obtained for the 45 steel (Fig. 4) is similar to those of the Armco iron (Fig. 3). Average increment of the specimen elongation for the plastic flow range has been about 1%. Beginning of the acoustic activity has been also observed in the elastic range of the specimen's deformation, like for the Armco iron. The only difference is that comparing to the lower bound of the yield limit, acoustic activity of the 45 carbon steel appears for higher stress than the approriate stress registered for the Armco iron. Greater number of the maximum and minimum points on the *RMS* curve has been observed within the Lüders platform and faster decrease of the acoustic activity within the hardening range has been noticed.

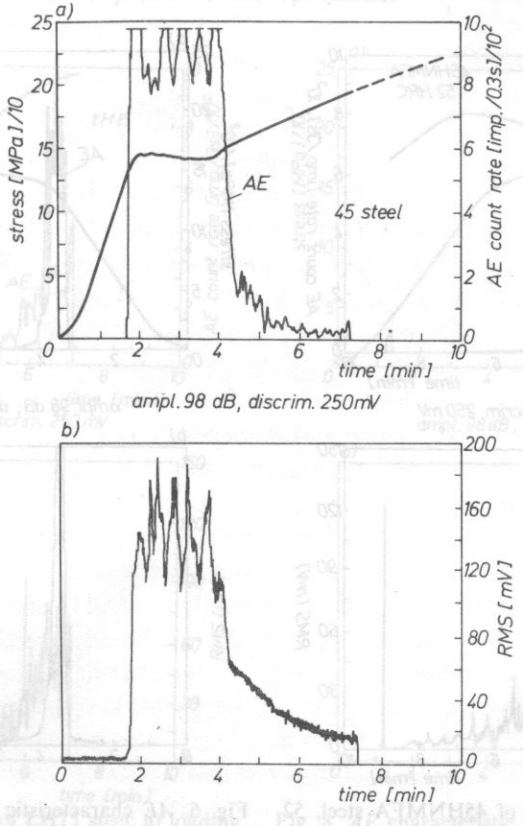

Fig. 4. *AE* characteristic of carbon steel 45

The lower bound of the yeld limit of the annealed 45 steel is approximately 2 times greater than the same bound of the Armco iron. The total elongation of the 45 steel specimens has been about 10% whereas the average reduction of the specimens area has been about 32%. Analogically as in the case of the Armco iron, the nature of the *AE* count rate is similar to the nature of the *RMS*. Initiation of the acoustic activity within the elastic deformation range and the cyclic change of this activity within the Lüders platform are the significant features of the 45 steel as well as Armco iron *AE* characteristic. The first feature gives evidence, that the range of the elastic deformation as estimated from the tension curve is elastic only in the conventional meaning. As a matter of fact, the irreversible changes of the material structure takes place even for this deformation. It leads to the energy release of the stressed specimen. Initiation of the plastic deformation registered by the *AE* method appears in the lower bound of yield limit.

3. 45HNMFA structural steel with the heat treatment on different hardness (52 and 42 HRC) has the characteristic typical for many policrystalline metals and alloys (Figs 5, 6). Acoustic activity of this steel contains in a narrow range of strain (except of the *RMS* curve of the 52 HRC hardness steel) and comes for the early beginning of

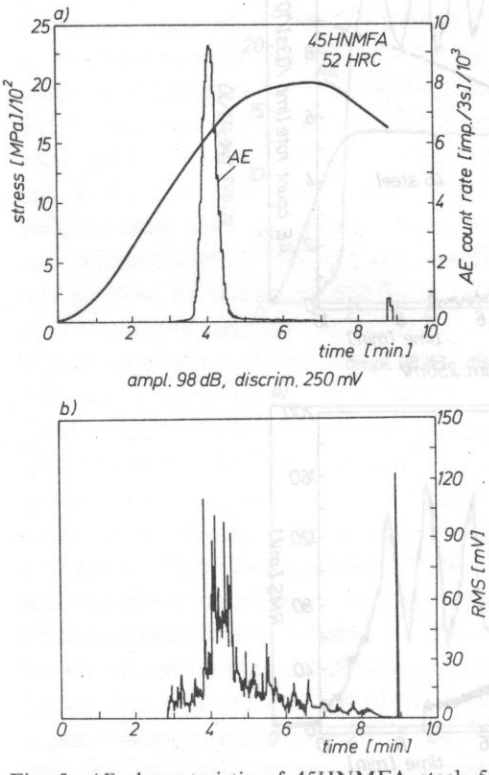

Fig. 5. *AE* characteristic of 45HNMFA steel, 52 HRC: a) loading curve and *AE* count rate: b) *RMS*

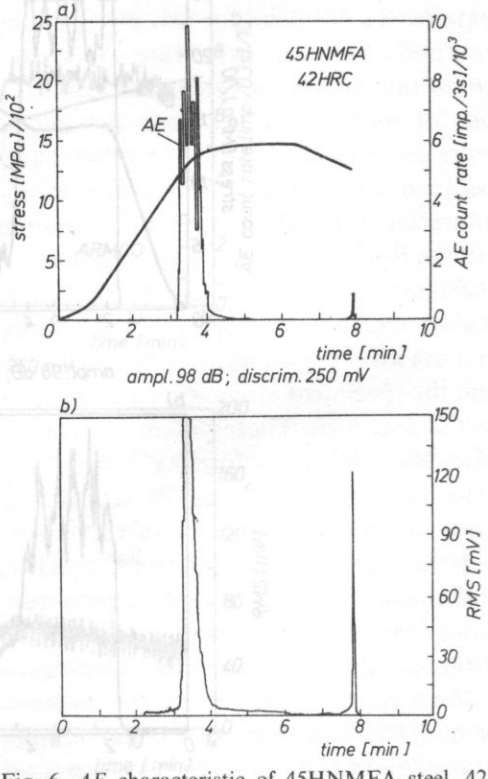

Fig. 6. *AE* characteristic of 45HNMFA steel, 42 HRC: a) loading curve and *AE* count rate; b) *RMS*

the hardening range. This steel does not exhibit the physical yield point. Significant differences of the count and event rate as well as *RMS* can be seen in *AE* characteristics of the 52 and 42 HRC hardness specimens. These differences give evidence of a different course of the plastic deformation process in the vicinity of the offset yield stress.

The *AE* count rate of the 52 HRC hardness steel grows and decreases monotonically and a curve appears in a triangular form. In the case of the 42 HRC hardness steel, significant fluctuations of the *AE* counts density is observed. Situation is just opposite if the *RMS* curves of the two varieties of this steel is taken into account (Figs 5 and 6). The acoustic activity level of the 45 HNMFA steel is lower than annealed Armco iron or 45 carbon steel.

4. ŁH15 bearing steel in the thermally treated and low-temperature tempering state exhibits different shape of the tension curve (lack of necking) as well as different character of the acoustic effect (Fig. 7). Immediate strength of this steel is very high (about 2500 MPa) whereas its irreversible elongation and cross area reduction measured in a plane of fracture are transiently small. Count rate and *RMS* appear in the vicinity of the offset yield point. Their growth is initially slow and grows with the load increase to the final repture of the specimen.

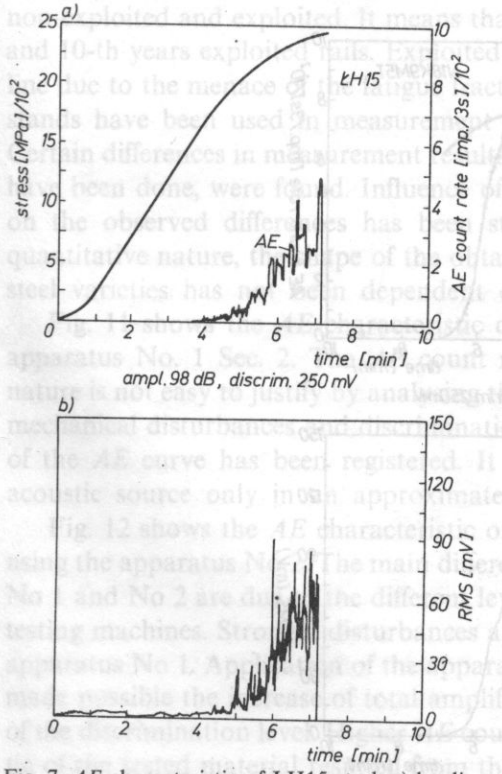

Fig. 7. *AE* characteristic of ŁH15 steel: a) loading curve and *AE* count rate; b) *RMS*

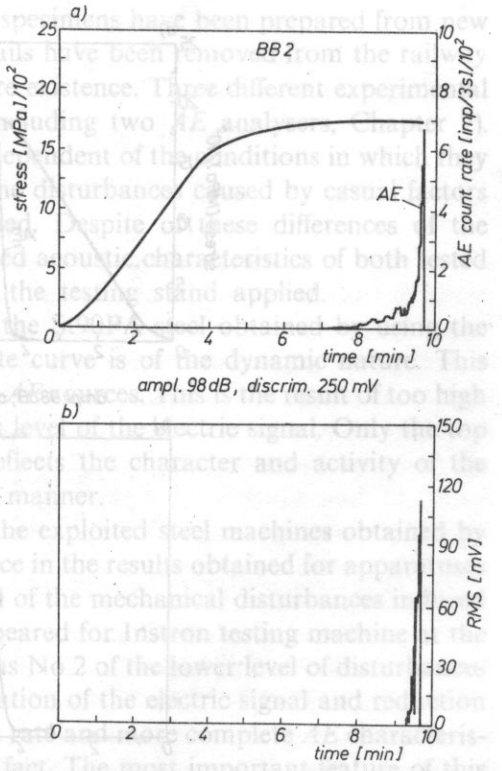

Fig. 8. *AE* characteristic of BB2 alloy: a) loading curve and *AE* count rate; b) *RMS*

5. BB2 beryllium bronze (Fig. 8) in the state after supersaturation and ageing has the most atypical *AE* characteristic of all the tested material although its tension curve is entirely typical. Acoustic effect appears only for the final phase of the specimen's tension process, just before its rupture. These is no acoustic activity in the hardening range of the material. Similarly as it was in the case of the bearing steel, also here these is no neck in the specimen and its cross area contraction is transiently small.

6. N18K9M5T maraging type alloy exhibits relatively high *AE* within all the range of plastic deformations (Fig. 9). Maximum activity coincides with the maximum point of the tension curve. Acoustic effect appears for load similar to the offset yield strength and grows monotonically within all the hardening range. In the range approximate for necking it grows small but remains perceptible to the final repture of the specimen.

7. PA2N aluminium alloy. *AE* of the PA2N alloy in the state hardened by cold working is typical (Fig. 10). Acoustic activity appears in the beginning of hardening. In the qualitative sense it can be compared with the *AE* characteristic of the 45HNMFA steel of the hardness equal 52HRC (Fig. 5). In the quantitative sense significant differences between both materials are manifested. These differences have

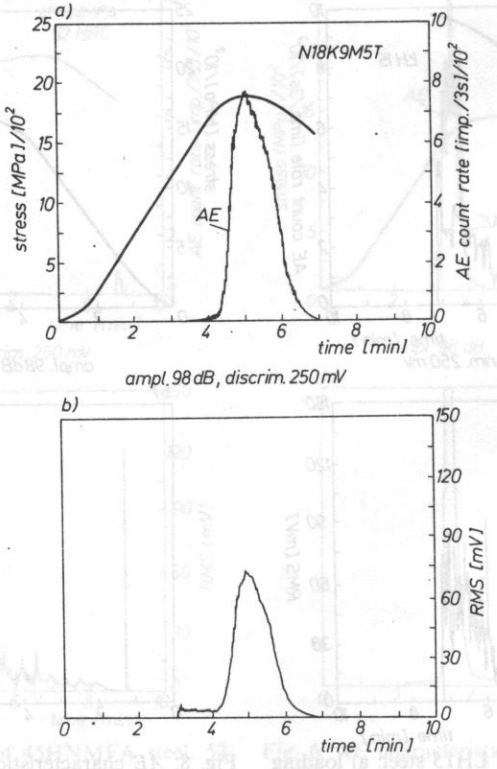

Fig. 9. *AE* characteristic of N18K9M5T alloy: a) loading curve and *AE* count rate; b) *RMS*

their reason both in different laboratory equipment used in test and in structural differences of both materials. The differences reflect in different acoustic effects for tentative loading conditions.

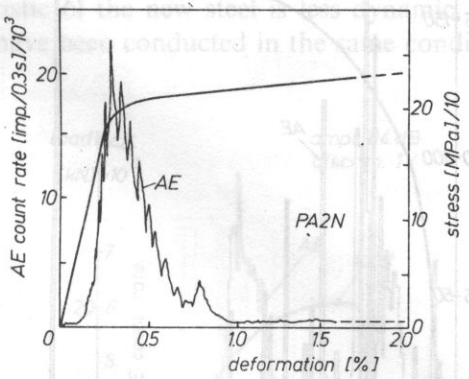

Fig. 10. *AE* characteristic of aluminium alloy PA2N after cold-working

8. St90PA carbon manganese steel has been tested in two varieties, that is non-exploited and exploited. It means that specimens have been prepared from new and 10-th years exploited rails. Exploited rails have been removed from the railway line due to the menace of the fatigue fracture existence. Three different experimental stands have been used in measurement (including two *AE* analysers, Chapter 2). Certain differences in measurement results dependent of the conditions in which they have been done, were found. Influence of the disturbances caused by casual factors on the observed differences has been stated. Despite of these differences of the quantitative nature, the shape of the obtained acoustic characteristics of both tested steel varieties has not been dependent of the testing stand applied.

Fig. 11 shows the *AE* characteristic of the St90PA steel obtained by using the apparatus No. 1 Sec. 2. The *AE* count rate curve is of the dynamic nature. This nature is not easy to justify by analysing the *AE* sources. This is the result of too high mechanical disturbances and discrimination level of the electric signal. Only the top of the *AE* curve has been registered. It reflects the character and activity of the acoustic source only in an approximated manner.

Fig. 12 shows the *AE* characteristic of the exploited steel machines obtained by using the apparatus No 2. The main difference in the results obtained for apparatuses No 1 and No 2 are due to the different level of the mechanical disturbances induced testing machines. Stronger disturbances appeared for Instron testing machine at the apparatus No 1. Application of the apparatus No 2 of the lower level of disturbances made possible the increase of total amplification of the electric signal and reduction of the discrimination level. Higher *AE* count rate and more complete *AE* characteristic of the tested material resulted from this fact. The most important feature of this characteristic is the distinctly marked shape of the area below the *AE* count rate

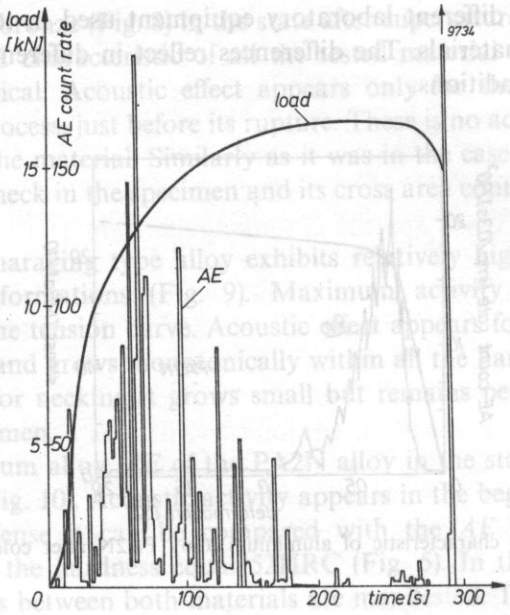

Fig. 11. *AE* characteristic of St90PA steel for tensile test on the test stand No 1. decreased amplification and increased discrimination level

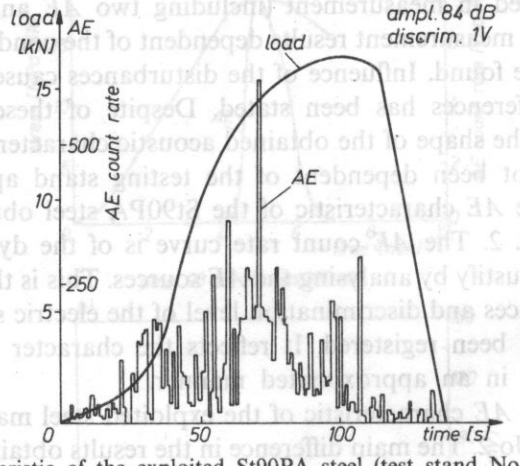

Fig. 12. *AE* characteristic of the exploited St90PA steel (test stand No 2. *AE* analyser *E*1)

curve. Evaluation of the source character is based on this shape. Initiation of the phenomenon appears when offset yield limit $\sigma_{0.2}$ is reached. For the exploited material this limit has been equal to 5 MPa and the value approximate the new material has been about 7 MPa. *AE* count rate rapidly grows and reaches maximum at the 2/3 of the hardening range. Then it grows small with the rate several times

smaller comparing to the grow rate. Acoustic effect accompanies the deformation of the specimen to its rupture. Dynamic character of the *AE* count rate well as acoustic activity existing within all the range of the plastic deformation of the material proves the existence of the strong jump internal reactions of the deforming material.

The *AE* characteristic of the new steel is less dynamic, Fig. 13. Measurements done for a new steel have been conducted in the same conditions as applied for the

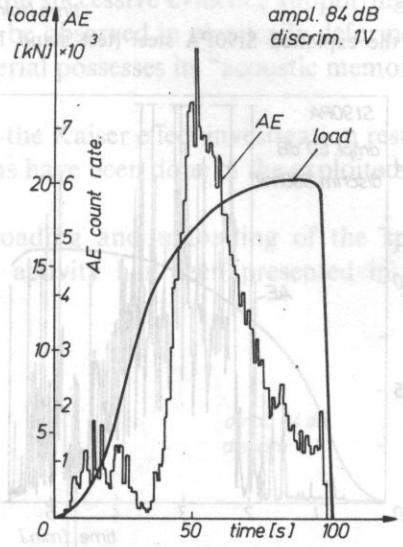

Fig. 13. *AE* characteristic of the new St90PA steel (test stand No 2. *AE* analyser *E*1)

exploited material, Fig. 12. The count rate graph is in the qualitative sense as the same the graph described above. Apparent quantitative differences consist in about 10 times greater acoustic activity, significantly marked characteristic and lower dynamic (nonhomogenity) of the *AE* count rate curve. Beginning of tension is accompanied by disturbances resulting from the arranging of the specimen ends in special catch handles and are not connected with the proper acoustic of the material.

Characteristics of the exploited and not exploited steel obtained by using the set-up No 3 with the DEMA-10 analyser are shown in Figs 14 and 15. None disturbances have been present here and the results have been registered by the *y–t* plotter. Both results have been obtained for the same measuring conditions which, in term, differ from the conditions of the set-up No 2 by the value amplification and the voltage of the discrimination level. Differences result from the requirements of the register installation. The qualitative changes of the *AE* count rate obtained by use of the two sets are nearly the same. It gives arguments for the appropriateness of the applied equipment and testing techniques. The *AE* in bending (Fig. 16) is generally similar to the characteristic obtained in tension (Fig. 13). On the other hand, determination of the peculiar points of the bending curve is more difficult. It leads to

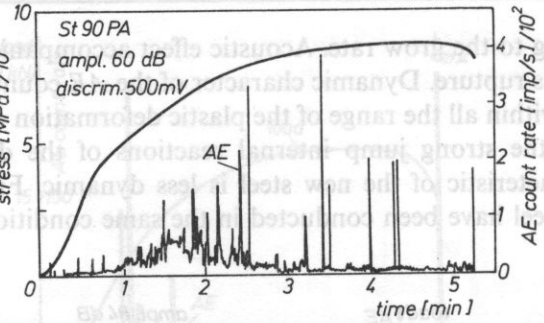

Fig. 14. *AE* characteristic of the exploited St90PA steel (test stand No 3, *AE* analyser *DEMA*-10)

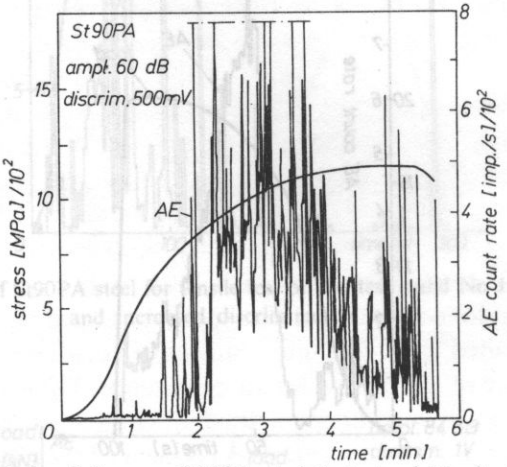

Fig. 15. *AE* characteristic of the new St90PA steel (test stand No 3, *AE* analyser *DEMA*-10)

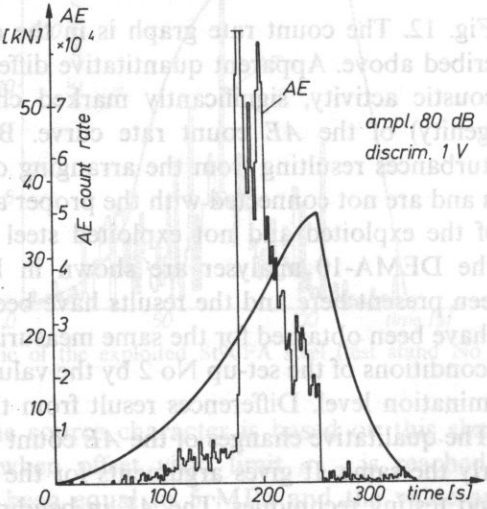

Fig. 16. *AE* characteristic of St90PA steel in bending (test stand No 1)

the certain difficulties in identification of the level of material deformation with the adequate acoustic effect. This effect is also connected with the existence of nonhomogeneous stresses inside the bended specimen that is with the simultaneous existence of compression and tensional stresses within the sample.

5. The Kaiser effect

The Kaiser effect is the successive evidence supporting the statement that certain irreversible changes can be observed in plastically deformed material. It also justifies the hypothesis that material possesses its "acoustic memory" of the loads it had been subjected in the past.

Figs 17 and 18 show the Kaiser effect investigation results obtained for specimens in tension. The specimens have been done of the exploited and non-exploited St90PA steel.

Example of triple loading and unloading of the specimen together with the accompanying acoustic activity has been presented in Fig. 19 to show that the

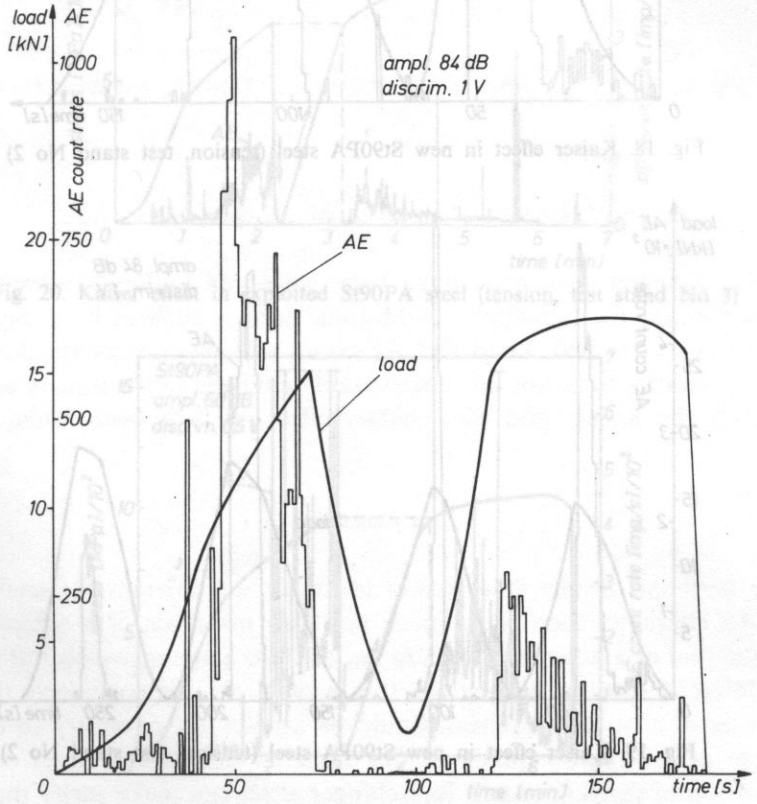

Fig. 17. Kaiser effect in exploited St90PA steel (tension, test stand No 2)

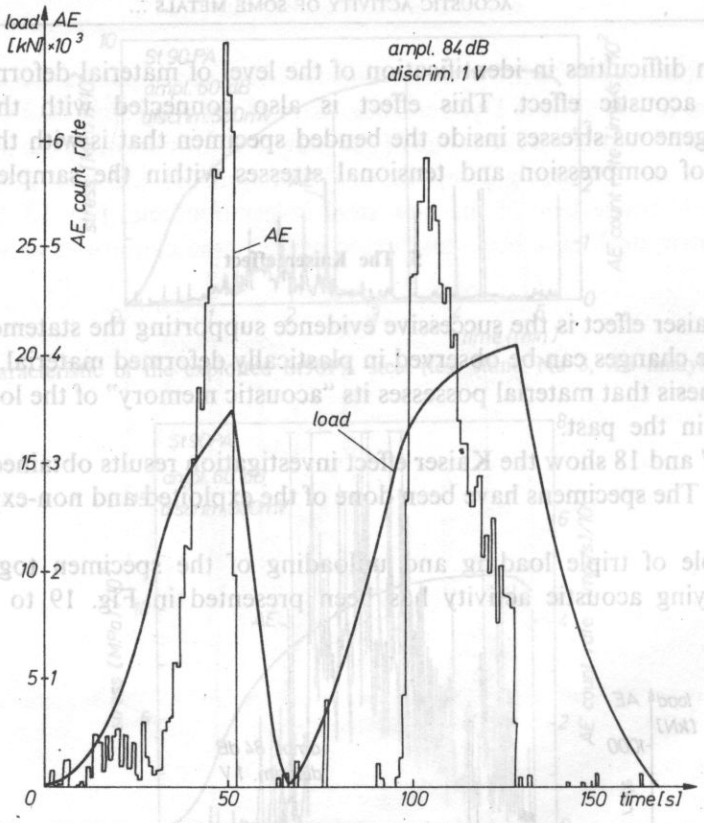

Fig. 18. Kaiser effect in new St90PA steel (tension, test stand No 2)

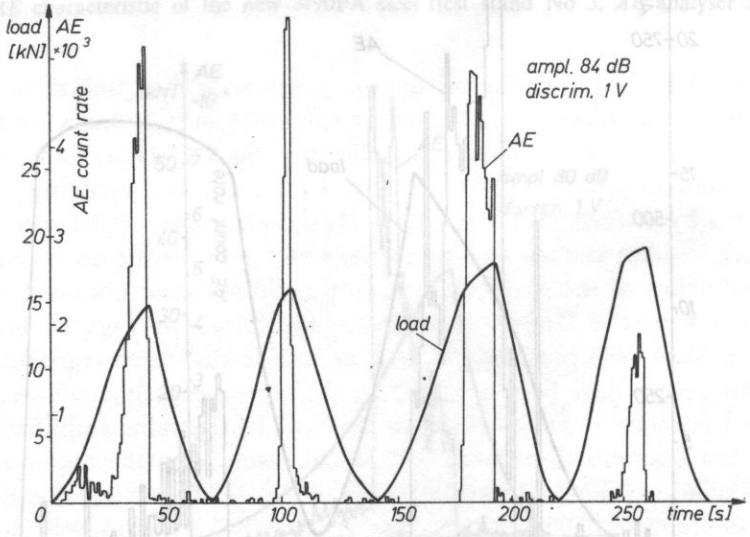

Fig. 19. Kaiser effect in new St90PA steel (tension, test stand No 2)

process does not depend on the stress value for which unloading begins and to show reliability of the material memory. We must notice that *AE* intensity reached for the moment of recovering activity in new loading is the same as it had been for the moment of unloading.

The results of the Kaiser effect measurements performed by using the set-up No. 3 are shown in Figs. 20 and 21. As before, also here they are all characterized by a very good repeatability. It can be seen that St90PA steel exhibits significant Kaiser effect for its both tested varieties. This effect establishes the certain kind of the material load memory and for this reason it makes possible the control of the loads applied in the past. It happens if the acoustic image is out disturbed by such sources of *AE* as the crack propagation or phase transitions. On the other hand, when the maximum level of the load applied is known, it forms a convenient background for controlling growth of dangerous processes leading to fracture.

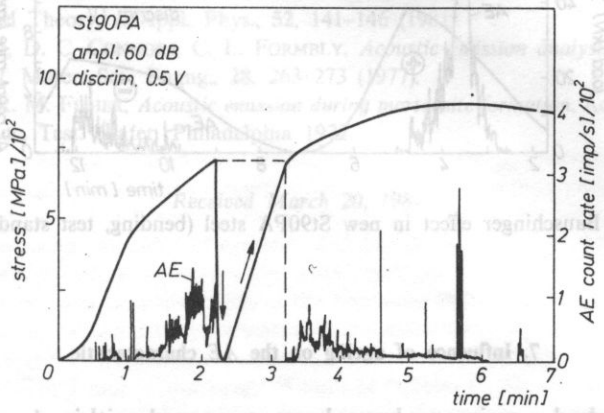

Fig. 20. Kaiser effect in exploited St90PA steel (tension, test stand No 3)

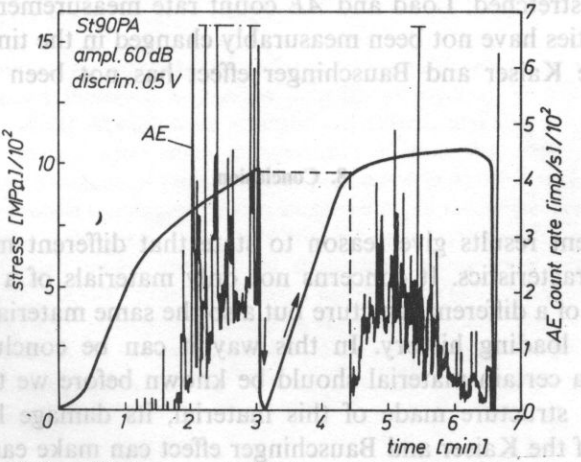

Fig. 21. Kaiser effect in new St90PA steel (tension, test stand No 3)

6. Bauschinger effect

Bauschinger effect has been confirmed much earlier than *AE* phenomenon was discovered. This effect concerns certain characteristic mechanical properties of the material. It consists in the reduction of the yield limit in metals due to their earlier plastic strain. Result of the *AE* count rate measurement in 3-point bending is shown in Fig. 22. The left-hand side of the figure (plus) concerns bending into one side whereas the right-hand side (minus) concerns bending of the same specimen but into other side. The result confirms existence of the phenomena accompanying it. The acoustic effect observed for second bending is much weaker out it is characterized by nearly constant level of activity.

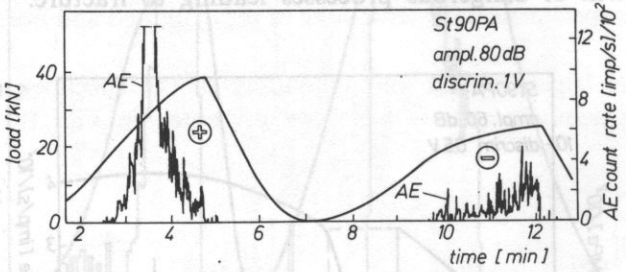

Fig. 22. Bauschinger effect in new St90PA steel (bending, test stand No 2)

7. Influence of ageing on the *AE* characteristic

Initially stretched specimens have been preserved within 1 month in natural conditions without the influence of additional factors such as humidity. Next they have been again stretched. Load and *AE* count rate measurements allow us to say that these quantities have not been measurably changed in the time of ageing. Effect of ageing on the Kaiser and Bauschinger effect has not been found also.

8. Conclusion

The experiment results give reason to state that different materials have very different *AE* characteristics. It concerns not only materials of a different chemical composition and of a different structure but also the same materials but heat treated or of a different loading history. In this way it can be concluded that the *AE* characteristic of a certain material should be known before we try to estimate the actual state of a structure made of this material, its damage level etc.

Application of the Kaiser and Bauschinger effect can make easier the estimation of maximum load that has acted on the structure in the past.

References

[1] S. PILECKI, *Wykorzystanie emisji akustycznej w badaniach własności mechanicznych i pękania ciał stałych*, Arch. Akust., **21**, 109 (1986).

[2] J. EISENBLÄTTER, J. BRECHT, P. JAX, *Werkstoffprüfung mit der Schallemissionanalyse*, Zeitsch. Werstofftechnik, 4, 306 (1973).

[3] H. JÖST, *Schallemissionsmessungen an bruchmechanischen Proben während wechselnder und zügiger Belastung*, Schallemission. DGM, München, April 1974, 149–169.

[4] C. B. SCRUBY, J. C. COLLINGWOOD, H. N. G. WADLEY, *A new technique for the measurement of acoustic emission transients and their relationship of crack propagation*, J. Appl. Phys. D., **11** (1978).

[5] F. HAMEL, J. P. BAILON, M. N. BASSIM, *Acoustic emission mechanism during high – cycle fatigue*, Eng. Fract. Mech., **14**, No 1, (1981).

[6] D. E. MACHA, D. M. CORBHY, I. W. JONES, *On the variation of fatigue crack – opening load with measurement location*, Exper. Mech., **19**, No 6 (1979).

[7] S. PILECKI, *Dislocation-diffusion mechanism of fatigue crack formation*, Fracture Vol. 2 ICF4 Waterloo, Canada, 1977, 687–693.

[8] R. A. KLINE, R. E. GREEN, C. H. PALMER, *Acoustic emission wave forms from cracking steel*, Experiment and Theory, J. Appl. Phys., **52**, 141–146 (1981).

[9] A. C. SINCLAIR, D. C. CONNORS, C. L. FORMBLY, *Acoustic emission analysis during fatigue crack growth in steel*. Mater. Sci., Engng., **28**, 263–273 (1977).

[10] G. R. SPEICH, R. M. FISHER, *Acoustic emission during martensite formation*, Acoustic Emission, STP – 505 Am. Soc. Test. Mater. Philadelphia 1972.

Received March 20, 1987